



The Thomas Jefferson National Accelerator Facility
Theory Group Preprint Series

JLAB-THY-01-08

Additional copies are available from the authors.

The Southeastern Universities Research Association (SURA) operates the Thomas Jefferson National Accelerator Facility for the United States Department of Energy under contract DE-AC05-84OR40150.

The hep Astrophysical Factor

R. Schiavilla
Jefferson Lab, Newport News, Virginia 23606
and
Department of Physics, Old Dominion University, Norfolk, Virginia 23529

The S -factor for the ${}^3\text{He}(p,e^+\nu_e){}^4\text{He}$ reaction has been recently calculated using realistic interactions and currents. The present talk summarizes the main results of that calculation.

1 Introduction

The present talk summarizes the salient points in a calculation of the astrophysical factor of the ${}^3\text{He}(p,e^+\nu_e){}^4\text{He}$ reaction, that was completed last year^{1,2}. Recently, there has been a revival of interest in the hep reaction^{3,4,5,6,7,8}, as the proton weak capture on ${}^3\text{He}$ is known. This interest has been spurred by the Super-Kamiokande collaboration measurements of the energy spectrum of electrons recoiling from scattering with solar neutrinos^{9,10,11}. Over most of the spectrum, a suppression $\simeq 0.5$ is observed relative to the Standard Solar Model (SSM) predictions¹². Above 12.5 MeV, however, there is an apparent excess of events. The hep process is the only source of solar neutrinos with energies larger than about 14 MeV—their end-point energy is about 19 MeV. This fact has naturally led to questions about the reliability of calculations of the hep weak capture cross section, upon which is based the currently accepted SSM value for the astrophysical S -factor at zero energy, 2.3×10^{-20} keV b¹³. In particular, Bahcall and Krastev have shown³ that a large enhancement, by a factor in the range 25–30, of the SSM S -factor value given above would essentially fit the observed excess⁹ of recoiling electrons, in any of three different neutrino scenarios—uniform suppression of the ${}^8\text{B}$ flux, vacuum oscillations, and matter-enhanced oscillations¹⁴.

The theoretical description of the hep process, as well as that of the neutron and proton radiative captures on ${}^2\text{H}$, ${}^3\text{H}$, and ${}^3\text{He}$, constitute a challenging problem from the standpoint of nuclear few-body theory. Its difficulty can be appreciated by comparing the measured values for the cross section of thermal neutron radiative capture on ${}^1\text{H}$, ${}^2\text{H}$, and ${}^3\text{He}$. Their respective values are: 334.2 ± 0.6 mb¹⁵, 0.508 ± 0.015 mb¹⁶, and 0.055 ± 0.003 mb^{17,18}. Thus, in going from $A=2$ to 4 the cross section has dropped by almost four orders of magnitude. These processes are induced by magnetic-dipole transitions between the initial two-cluster state in relative S -wave and the final bound

DISCLAIMER

This report was prepared as an account of work sponsored by the United States government. Neither the United States nor the United States Department of Energy, nor any of their employees, makes any warranty, expressed or implied, or assumes any legal liability or responsibility for the accuracy, completeness, or usefulness of any information, apparatus, product, or process disclosed, or represents that its use would not infringe privately owned rights. Reference herein to any specific commercial product, process, or service by trade name, mark, manufacturer, or otherwise, does not necessarily constitute or imply its endorsement, recommendation, or favoring by the United States government or any agency thereof. The views and opinions of authors expressed herein do not necessarily state or reflect those of the United States government or any agency thereof.

state. In fact, the inhibition of the $A=3$ and 4 captures has been understood for a long time¹⁹. The ^3H and ^4He wave functions, denoted, respectively, with Ψ_3 and Ψ_4 are, to a good approximation, eigenfunctions of the magnetic dipole operator μ , namely $\mu_x \Psi_3 \simeq \mu_p \Psi_3$ and $\mu_x \Psi_4 \simeq 0$, where $\mu_p = 2.793$ n.m. is the proton magnetic moment (note that the experimental value of the ^3H magnetic moment is 2.979 n.m., while ^4He has no magnetic moment). These relations would be exact, if the ^3H and ^4He wave functions were to consist of a symmetric S-wave term only, for example, $\Psi_4 = \phi_4(S) \det \{ p \uparrow_1, p \downarrow_2, n \uparrow_3, n \downarrow_4 \}$. Of course, tensor components in the nuclear interactions generate significant D-state admixtures, that partially spoil this eigenstate property. To the extent that it is approximately satisfied, though, the matrix elements $\langle \Psi_3 | \mu_x | \Psi_{1+2} \rangle$ and $\langle \Psi_4 | \mu_x | \Psi_{1+3} \rangle$ vanish due to orthogonality between the initial and final states. This orthogonality argument fails in the case of the deuteron, since then

$$\mu_x \Psi_2 \simeq (\mu_p - \mu_n) \phi_2(S) \chi_0^0 \eta_0^0, \quad (1)$$

where χ_0^0 and η_0^0 are two-nucleon spin and isospin states, respectively. The magnetic dipole operator can therefore connect the large S-wave component $\phi_2(S)$ of the deuteron to a $T=1$ $^3\text{S}_0$ np state (note that the orthogonality between the latter and the deuteron follows from the orthogonality between their respective spin-isospin states).

This quasi-orthogonality, while again invalid in the case of the proton weak capture on protons, is also responsible for inhibiting the hep process. Both these reactions are induced by the Gamow-Teller operator, which differs from the (leading) isovector spin part of the magnetic dipole operator essentially by an isospin rotation. As a result, the hep weak capture and nd , pd , $n^3\text{He}$, and $p^3\text{H}$ radiative captures are extremely sensitive to: (i) small components in the wave functions, particularly the D-state admixtures generated by tensor interactions, and (ii) many-body terms in the electro-weak current operator. For example, two-body current contributions provide, respectively, 50 % and over 90 % of the calculated pd ²⁰ and $n^3\text{He}$ ^{13,21} cross sections at very low energies.

In this respect, the hep weak capture is a particularly delicate reaction, for two additional reasons: firstly and most importantly, the one- and two-body current contributions are comparable in magnitude, but of opposite sign^{13,22}; secondly, two-body axial currents, specifically those arising from excitation of Δ isobars which have been shown to give the dominant contribution, are model dependent^{22,23,24}.

This destructive interference between one- and two-body currents also occurs in the $n^3\text{He}$ ("hen") radiative capture^{13,21}, with the difference that there

the leading components of the two-body currents are model independent, and give a much larger contribution than that associated with the one-body current.

The cancellation in the hep process between the one- and two-body matrix elements has the effect of enhancing the importance of P-wave capture channels, which would ordinarily be suppressed. Indeed, one of the results reported here is that these channels give about 40 % of the S-factor calculated value. That the hep process could proceed as easily through P- as S-wave capture was not realized—or, at least, not sufficiently appreciated²⁵—in all earlier studies of this reaction we are aware of, with the exception of Ref.⁶, where it was suggested, on the basis of a very simple one-body reaction model, that the $^3\text{P}_0$ channel may be important.

2 Interactions, Currents, and Wave Functions

Improvements in the modeling of two- and three-nucleon interactions and the nuclear weak current, and the significant progress made in the last few years in the description of the bound and continuum four-nucleon wave functions, have prompted us to re-examine the hep reaction^{1,2}. The nuclear Hamiltonian has been taken to consist of the Argonne v_{18} two-nucleon²⁷ and Urbana-IX three-nucleon²⁸ interactions. To make contact with the earlier studies^{13,22}, however, and to have some estimate of the model dependence of the results, the older Argonne v_{14} two-nucleon²⁹ and Urbana-VIII three-nucleon³⁰ interaction models have also been used. Both these Hamiltonians, the AV18/UIX and AV14/UVIII, reproduce the experimental binding energies and charge radii of the trinucleons and ^4He in exact Green's function Monte Carlo (GFMC) calculations^{31,32}.

The correlated-hyperspherical-harmonics (CHH) method is used here to solve variationally the bound- and scattering-state four-nucleon problem^{33,34}. The binding energy of ^4He calculated with the CHH method^{33,36} is within 1-2 %, depending on the Hamiltonian model, of that obtained with the GFMC method. The accuracy of the CHH method to calculate scattering states has been successfully verified in the case of the trinucleon systems, by comparing results for a variety of Nd scattering observables obtained by a number of groups using different techniques³⁵. Indeed, the numerical uncertainties in the calculation of the trinucleon continuum have been so drastically reduced that Nd scattering observables can now be used to directly study the sensitivity to two- and three-nucleon interaction models—the A_p "puzzle" constitutes an excellent example of this type of studies³⁷.

Studies along similar lines show³⁸ that the CHH solutions for the four-

nucleon continuum are also highly accurate. The CHH predictions³⁴ for the n ^3H total elastic cross section, $\sigma_T = \pi (|a_s|^2 + 3|a_t|^2)$, and coherent scattering length, $a_c = a_s/4 + 3a_t/4$, measured by neutron interferometry techniques— a_s and a_t are the singlet and triplet scattering lengths—have been found to be in excellent agreement with the corresponding experimental values. The n ^3H cross section is known over a rather wide energy range, and its extrapolation to zero energy is not problematic³². The situation is different for the p ^3He channel, for which the scattering lengths have been determined from effective range extrapolations of data taken above 1 MeV, and are therefore somewhat uncertain, $a_s = (10.8 \pm 2.0)$ fm⁴⁰ and $a_t = (8.1 \pm 0.5)$ fm⁴⁰ or (10.2 ± 1.5) fm²⁵. Nevertheless, the CHH results are close to the experimental values above. For example, the AV18/UIX Hamiltonian predicts³⁴ $a_s = 10.1$ fm and $a_t = 9.13$ fm.

In Refs.^{13,22} variational Monte Carlo (VMC) wave functions had been used to describe both bound and scattering states. The triplet scattering length was found to be 10.1 fm with the AV14/UVIII Hamiltonian model, in satisfactory agreement with the experimental determination and the value obtained with the more accurate CHH wave functions. However, the present work includes all S- and P-wave channels, namely 1S_0 , 3S_1 , 3P_0 , 1P_1 , 3P_1 , and 3P_2 , while all previous works only retained the 3S_1 channel, which was thought, erroneously, to be the dominant one.

The nuclear weak current consists of vector and axial-vector parts, with corresponding one-, two-, and many-body components. The weak vector current is constructed from the isovector part of the electromagnetic current, in accordance with the conserved-vector-current (CVC) hypothesis. Two-body weak vector currents have model-independent and model-dependent components. The model-independent terms are obtained from the nucleon-nucleon interaction, and by construction satisfy current conservation with it. The leading two-body weak vector current is the " π -like" operator, obtained from the isospin-dependent spin-spin and tensor nucleon-nucleon interactions. The latter also generate an isovector " ρ -like" current, while additional isovector two-body currents arise from the isospin-independent and isospin-dependent central and momentum-dependent interactions. These currents are short-ranged, and numerically far less important than the π -like current. With the exception of the ρ -like current, they have been neglected in the present work. The model-dependent currents are purely transverse, and therefore cannot be directly linked to the underlying two-nucleon interaction. The present calculation includes the isovector currents associated with excitation of Δ isobars which, however, are found to give a rather small contribution in weak-vector transitions, as compared to that due to the π -like current. The π -like and ρ -like

weak vector charge operators have also been retained in the present study.

The leading two- and many-body terms in the axial current, in contrast to the case of the weak vector (or electromagnetic) current, are those due to Δ -isobar excitation, which are treated within the transition-correlation-operator (TCO) scheme. The TCO method—a scaled-down approach to a full $N + \Delta$ coupled-channel treatment—includes the Δ degrees of freedom explicitly in the nuclear wave functions. The axial charge operator includes the long-range pion-exchange term⁴¹, required by low-energy theorems and the partially-conserved-axial-current relation, as well as the (expected) leading short-range terms constructed from the central and spin-orbit components of the nucleon-nucleon interaction, following a prescription due to Kirchbach *et al.*⁴².

The largest model dependence is in the weak axial current. To minimize it, the poorly known $N \rightarrow \Delta$ transition axial coupling constant has been adjusted to reproduce the experimental value of the Gamow-Teller matrix element in tritium β -decay. While this procedure is inherently model dependent, its actual model dependence is in fact very weak, as has been shown in Ref. 43. The analysis carried out there could be extended to the present case.

3 Results for the hep S -Factor

Our results for the astrophysical S -factor, as function of the center-of-mass energy E , are reported in Table 1. By inspection of the table, we note that: (i) the energy dependence is rather weak: the value at 10 keV is only about 4 % larger than that at 0 keV; (ii) the P-wave capture states are found to be important, contributing about 40 % of the calculated S -factor. However, the contributions from D-wave channels are expected to be very small. We have verified explicitly that they are indeed small in $^3\text{D}_1$ capture. (iii) The many-body axial currents associated with Δ excitation play a crucial role in the (dominant) 3S_1 capture, where they reduce the S -factor by more than a factor of four; thus the destructive interference between the one- and many-body current contributions, first obtained in Ref. 22, is confirmed in the present study, based on more accurate wave functions. The (suppressed) one-body contribution comes mostly from transitions involving the D-state components of the ^3He and ^4He wave functions, while the many-body contributions are predominantly due to transitions connecting the S-state in ^3He to the D-state in ^4He , or viceversa. It is important to stress the differences between the present and all previous studies. Apart from ignoring, or at least underestimating, the contribution due to P-waves, the latter only considered the long-wavelength form of the weak multipole operators, namely, their $q=0$ limit, where q is the magnitude of the momentum transfer. In $^3\text{P}_0$ capture, for example, only the

Table 1: The hep S -factor, in units of 10^{-20} keV b, calculated with CHH wave functions corresponding to the AV18/UIX Hamiltonian model, at p ³He c.m. energies $E=0, 5,$ and 10 keV. The rows labeled "one-body" and "full" list the contributions obtained by retaining the one-body only and both one- and many-body terms in the nuclear weak current. The contributions due to the 3S_1 channel only and all S- and P-wave channels are listed separately.

	$E=0$ keV		$E=5$ keV		$E=10$ keV	
	3S_1	S+P	3S_1	S+P	3S_1	S+P
one-body	26.4	29.0	25.9	28.7	26.2	29.3
full	6.38	9.64	6.20	9.70	6.36	10.1

C_0 -multipole, associated with the weak axial charge, survives in this limit, and the corresponding S -factor is calculated to be 2.2×10^{-20} keV b, including two-body contributions. However, when the transition induced by the longitudinal component of the axial current (via the L_0 -multipole, which vanishes at $q=0$) is also taken into account, the S -factor becomes 0.82×10^{-20} keV b, because of destructive interference between the C_0 and L_0 matrix elements. Thus use of the long-wavelength approximation in the calculation of the hep cross section leads to inaccurate results.

Finally, besides the differences listed above, the present calculation also improves that of Ref. ¹³ in a number of other important respects: firstly, it uses CHH wave functions, corresponding to the latest generation of realistic interactions; secondly, the model for the nuclear weak current has been extended to include the axial charge as well as the vector charge and current operators. Thirdly, the one-body operators now take into account the $1/m^2$ relativistic corrections, which had previously been neglected. In 3S_1 capture, for example, these terms increase by 25 % the dominant (but suppressed) L_1 and E_1 matrix elements calculated with the (lowest order) Gamow-Teller operator. These improvements in the treatment of the one-body axial current indirectly affect also the contributions of the Δ -excitation currents, since the $N\Delta$ transition axial coupling constant is determined by reproducing the Gamow-Teller matrix element in tritium β -decay.

The chief conclusion of the present work is that the hep S -factor is predicted to be $\simeq 4.5$ times larger than the value adopted in the SSM. This enhancement, while very significant, is smaller than that first suggested in Refs. ^{3,5}, and then reconsidered by the SK collaboration in Ref. ¹¹. A discussion of the implications of our results for the SK solar neutrino spectrum is given below.

Even though our result is inherently model dependent, it is unlikely that

the model dependence is large enough to accommodate a drastic increase in the value obtained here. Indeed, calculations using Hamiltonians based on the AV18 two-nucleon interaction only and the older AV14/UVIII two- and three-nucleon interactions predict² zero energy S -factor values of 12.1×10^{-20} keV b and 10.2×10^{-20} keV b, respectively. It should be stressed, however, that the AV18 model, in contrast to the AV14/UVIII, does not reproduce the experimental binding energies and low-energy scattering parameters of the three- and four-nucleon systems. The AV14/UVIII prediction is only 6 % larger than the AV18/UIX zero-energy result. This 6 % variation should provide a fairly realistic estimate of the theoretical uncertainty due to the model dependence.

To conclude, our best estimate for the S -factor at 10 keV c.m. energy is therefore $(10.1 \pm 0.6) \times 10^{-20}$ keV b.

4 Impact on the Super-Kamiokande Solar Neutrino Spectrum

Super-Kamiokande (SK) detects solar neutrinos by neutrino-electron scattering. The energy is shared between the outgoing neutrino and scattered electron, leading to a very weak correlation between the incoming neutrino energy and the measured electron energy. The electron angle relative to the solar direction is also measured, which would in principle allow reconstruction of the incoming neutrino energy. However, the kinematic range of the angle is very forward, and is comparable to the angular resolution of the detector. Furthermore, event-by-event reconstruction of the neutrino energy would be prevented by the detector background. Above its threshold of several MeV, SK is sensitive to the 8B electron neutrinos. These have a total flux of 5.15×10^6 cm⁻² s⁻¹ in the SSM¹². While the flux is uncertain to about 15 %, primarily due to the nuclear-physics uncertainties in the $^7Be(p,\gamma)^8B$ cross section, the spectral shape is more precisely known⁴⁴.

The SK results are presented as the ratio of the measured electron spectrum to that expected in the SSM with no neutrino oscillations. Over most of the spectrum, this ratio is constant at $\simeq 0.5$. At the highest energies, however, an excess relative to $0.5 \times$ SSM is seen (though it has diminished in successive data sets). The SK 825-day data, determined graphically from Fig. 8 of Ref. ¹¹, are shown by the points in Fig. 1 (the error bars denote the combined statistical and systematic error). The excess above 12.5 MeV may be interpreted as neutrino-energy dependence in the neutrino oscillation probability that is not completely washed out in the electron spectrum. This excess has also been interpreted as possible evidence for a large hep flux^{3,5,11} (though note that the data never exceeds the full SSM expectation from 8B neutrinos). In the

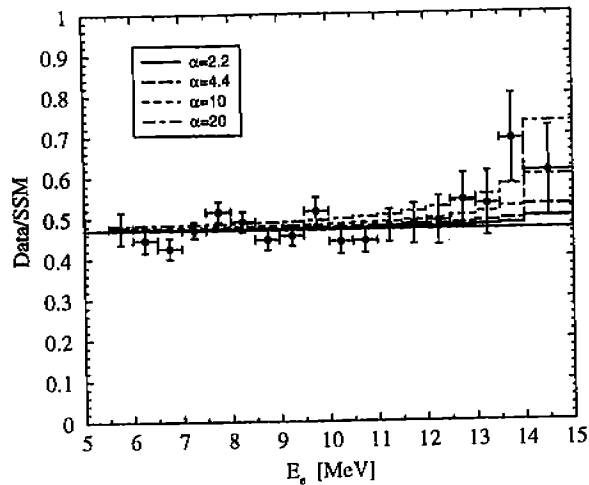


Figure 1: Electron energy spectrum for the ratio between the Super-Kamiokande 825-days data and the expectation based on unoscillated ^8B neutrinos¹². The data were extracted graphically from Fig. 8 of Ref. ¹¹. The 5 curves correspond respectively to no ^8B contribution, and an enhancement α of 2.2, 4.4, 10 and 20.

SSM, the total ^8B flux is very small, $2.10 \times 10^3 \text{ cm}^{-2} \text{ s}^{-1}$. However, its endpoint energy is higher than for the ^8B neutrinos, 19 MeV instead of about 14 MeV, so that the ^8B neutrinos may be seen at the highest energies. This is somewhat complicated by the energy resolution of SK, which allows ^8B events beyond their nominal endpoint. The ratio of the ^8B flux to its value in the SSM (based on the ^8B S-factor prediction of Ref. ¹³) will be denoted by α , defined as

$$\alpha \equiv \frac{S_{\text{new}}}{S_{\text{SSM}}} \times P_{\text{osc}}, \quad (2)$$

where P_{osc} is the ^8B -neutrino suppression constant. In the present work, $\alpha = (10.1 \times 10^{-20} \text{ keV b}) / (2.3 \times 10^{-20} \text{ keV b}) = 4.4$, if ^8B neutrino oscillations are ignored. The lines in Fig. 1 indicate the effect of various values of α on the ratio of the electron spectrum with both ^8B and ^8He to that with only ^8B (the SSM). Though some differences are expected in the ^8B spectral shape due to P-wave contributions, here we simply use the standard ^8B spectrum shape⁴⁵. In calculating this ratio, the ^8B flux in the numerator has been suppressed by 0.47, the best-fit constant value for the observed suppression. If the ^8B neutrinos are suppressed by ≈ 0.5 , then $\alpha = 2.2$. Two other arbitrary values of α (10 and 20) are shown for comparison. As for the SK data, the results are shown as a function of the total electron energy in 0.5 MeV bins. The last bin, shown covering 14 - 15 MeV, actually extends to 20 MeV. The SK energy resolution was approximated by convolution with a Gaussian of energy-dependent width, chosen to match the SK LINAC calibration data⁴⁶.

The effects of a larger ^8B flux should be compared to other possible distortions of the ratio. The data show no excess at low energies, thus limiting the size of a neutrino magnetic moment contribution to the scattering⁴⁷. The ^8B neutrino energy spectrum has recently been remeasured by Ortiz *et al.*⁴⁸ and their spectrum is significantly larger at high energies than that of Ref. ⁴⁴. Relative to the standard spectrum, this would cause an increase in the ratio at high energies comparable to the $\alpha = 4.4$ case. The measured electron spectrum is very steep, and the fraction of events above 12.5 MeV is only $\sim 1\%$ of the total above threshold. Thus, an error in either the energy scale or resolution could cause an apparent excess of events at high energy. However, these are known precisely from the SK LINAC⁴⁶ calibration; an error in either could explain the data only if it were at about the 3- or 4-sigma level¹¹.

The various neutrino oscillation solutions can be distinguished by their neutrino-energy dependence, though the effects on the electron spectrum are small. Generally, the ratio is expected to be rising at high energies, much like the effect of an increased ^8B flux. The present work predicts $\alpha = 4.4$ (and $\alpha = 2.2$ if the ^8B neutrinos oscillate). From Fig. 1, this effect is smaller than the distortion seen in the data or found in Refs. ^{3,5,11}, where the ^8B flux was fitted as a free parameter. However, the much more important point is that this is an *absolute* prediction. Fixing the value of α will significantly improve the ability of SK to identify the correct oscillation solution. In this context, we refer the reader to the report by Smy⁴⁹ in these proceedings, for the most recent release and analysis of data from the SK collaboration.

5 Acknowledgments

I wish to thank L.E. Marcucci, M. Viviani, A. Kievsky, S. Rosati, and J.F. Beacom for their many important contributions to the work reported here. This project was supported by DOE Contract No. DE-AC05-84ER40150 under which the Southeastern Universities Research Association operates the Thomas Jefferson National Accelerator Facility.

References

1. L.E. Marcucci, R. Schiavilla, M. Viviani, A. Kievsky, and S. Rosati, *Phys. Rev. Lett.* **84**, 5959 (2000).
2. L.E. Marcucci, R. Schiavilla, M. Viviani, A. Kievsky, S. Rosati, and J.F. Beacom, *Phys. Rev. C* **63**, 015801 (2001).
3. J.N. Bahcall and P.I. Krastev, *Phys. Lett. B* **436**, 243 (1998).
4. G. Fiorentini, V. Berezinsky, S. Degl'Innocenti, and B. Ricci, *Phys. Lett. B* **444**, 387 (1998).
5. R. Escribano, J.M. Frère, A. Gevaert, and P. Monderen, *Phys. Lett. B* **444**, 397 (1998).
6. C.J. Horowitz, *Phys. Rev. C* **60**, 022801 (1999).
7. W.M. Alberico, S.M. Bilenky, and W. Grimus, hep-ph/0001245.
8. W.M. Alberico, J. Barnabéu, S.M. Bilenky, and W. Grimus, *Phys. Lett. B* **478**, 208 (2000).
9. Y. Fukuda *et al.*, *Phys. Rev. Lett.* **82**, 2430 (1999).
10. M.B. Smy, hep-ex/9903034.
11. Y. Suzuki, contribution to Lepton-Photon Symposium 99 (1999), <http://www-sk.icrr.u-tokyo.ac.jp/doc/sk/pub/index.html>.
12. J.N. Bahcall, S. Basu, and M.H. Pinsonneault, *Phys. Lett. B* **433**, 1 (1998).
13. R. Schiavilla, R.B. Wiringa, V.R. Pandharipande, and J. Carlson, *Phys. Rev. C* **45**, 2628 (1992).
14. S.P. Mikheev and A.Y. Smirnov, *Nuovo Cim.* **9C**, 17 (1986).
15. A.E. Cox, S.A.R. Wynchank, and C.H. Collie, *Nucl. Phys.* **74**, 497 (1965).
16. E.T. Jurney, P.J. Bondt, and J.C. Browne, *Phys. Rev. C* **25**, 2810 (1982).
17. F.L.H. Wolfs, S.J. Freedman, J.E. Nelson, M.S. Dewey, and G.L. Greene, *Phys. Rev. Lett.* **63**, 2721 (1989).
18. R. Wervelmann, K. Abrahams, H. Postma, J.G.L. Booten, and A.G.M. Van Hess, *Nucl. Phys.* **A526**, 265 (1991).
19. L.I. Schiff, *Phys. Rev.* **52**, 242 (1937).
20. M. Viviani, A. Kievsky, L.E. Marcucci, S. Rosati, and R. Schiavilla, *Phys. Rev. C* **61**, 064001 (2000).
21. J. Carlson, D.O. Riska, R. Schiavilla, and R.B. Wiringa, *Phys. Rev. C* **42**, 830 (1990).
22. J. Carlson, D.O. Riska, R. Schiavilla, and R.B. Wiringa, *Phys. Rev. C* **44**, 619 (1991).
23. M. Chemtob and M. Rho, *Nucl. Phys.* **A163**, 1 (1971).
24. I.S. Towner, *Phys. Rep.* **155**, 263 (1987).
25. C. Werntz and J.G. Brennan, *Phys. Rev. C* **8**, 1545 (1973).
26. P.E. Tigner and C. Bargholtz, *Astrophys. J.* **272**, 311 (1983).
27. R.B. Wiringa, V.G.J. Stoks, and R. Schiavilla, *Phys. Rev. C* **51**, 38 (1995).
28. B.S. Pudliner, V.R. Pandharipande, J. Carlson, and R.B. Wiringa, *Phys. Rev. Lett.* **74**, 4396 (1995).
29. R.B. Wiringa, R.A. Smith, and T.L. Ainsworth, *Phys. Rev. C* **29**, 1207 (1984).
30. R.B. Wiringa, *Phys. Rev. C* **43**, 1585 (1991).
31. B.S. Pudliner, V.R. Pandharipande, J. Carlson, S.C. Pieper, and R.B. Wiringa, *Phys. Rev. C* **58**, 1720 (1997).
32. J. Carlson, private communication.
33. M. Viviani, A. Kievsky, and S. Rosati, *Few-Body Syst.* **18**, 25 (1995).
34. M. Viviani, S. Rosati, and A. Kievsky, *Phys. Rev. Lett.* **81**, 1580 (1998).
35. M. Viviani, private communication.
36. A. Kievsky *et al.*, *Phys. Rev. C* **58**, 3085 (1998).
37. W. Glöckle *et al.*, *Phys. Rep.* **274**, 107 (1996), and references therein; A. Kievsky, *Phys. Rev. C* **60**, 034001 (1999).
38. M. Viviani, *Nucl. Phys.* **A631**, 111c (1998).
39. T.W. Phillips, B.L. Berman, and J.D. Seagrave, *Phys. Rev. C* **22**, 384 (1980).
40. M.T. Alley and L.D. Knutson, *Phys. Rev. C* **48**, 1901 (1993).
41. K. Kubodera, J. Delorme, and M. Rho, *Phys. Rev. Lett.* **40**, 755 (1978).
42. M. Kirchbach, D.O. Riska, and K. Tsushima, *Nucl. Phys.* **A542**, 616 (1992).
43. R. Schiavilla *et al.*, *Phys. Rev. C* **58**, 1283 (1998).
44. J. N. Bahcall, E. Lisi, D.E. Alburger, L. De Braeckeleer, S.J. Freedman, and J. Napolitano, *Phys. Rev. C* **54**, 411 (1996).
45. <http://www.sns.ias.edu/~jnb>.
46. M. Nakahata *et al.*, *Nucl. Instrum. Methods Phys. Res., Sect. A* **421**, 113 (1999).
47. J.F. Beacom and P. Vogel, *Phys. Rev. Lett.* **83**, 5222 (1999).
48. C.E. Ortiz *et al.*, nucl-ex/0003006.
49. M.B. Smy, these proceedings.